hydrogen

MDPI

Communication

Simulation and Quantitative Assessment of Sensor Placement in a Hydrogen Bus for Risk Mitigation

Xintao Deng *, Jinwei Sun, Fuyuan Yang * and Minggao Ouyang

State Key Laboratory of Automotive Safety and Energy, School of Vehicle and Mobility, Tsinghua University, Beijing 100084, China; sjw@tsinghua.edu.cn (J.S.)

* Correspondence: dxt20@mails.tsinghua.edu.cn (X.D.); fyyang@tsinghua.edu.cn (F.Y.)

Abstract: The cleanliness of hydrogen energy throughout its life cycle has enabled its applications in transportation and buildings. However, such scenarios often involve the storage and use of hydrogen in enclosed spaces. Ensuring the facility's safety during hydrogen accidental leakage through rapid detection and emergency measures has been a long-standing topic. In this work, we analyze hydrogen leakage in a hydrogen bus through CFD simulation. By extracting the hydrogen diffusion time and combining it with the leakage frequency and ignition probability, we quantitatively evaluate the placement of the sensors and propose an index for detection system assessment named the average detection delay index (ADDI). A near-field detection sensor was introduced to the system, which reduced the lower ADDI limit of the detection system by up to 10 times while reducing the system cost without changing the level of performance.

Keywords: hydrogen safety; leakage detection; quantitative assessment; hydrogen sensor; numerical simulation

check for updates

Citation: Deng, X.; Sun, J.; Yang, F.; Ouyang, M. Simulation and Quantitative Assessment of Sensor Placement in a Hydrogen Bus for Risk Mitigation. *Hydrogen* **2024**, *5*, 976–986. https://doi.org/10.3390/hydrogen5040052

Academic Editor: Silvano Tosti

Received: 15 October 2024
Revised: 4 December 2024
Accepted: 4 December 2024
Published: 8 December 2024

1. Introduction

The world is embracing the large-scale application of hydrogen in electrical systems, transportation, and renewable energy storage. However, safety concerns still exist. Because of its small molecular volume, high calorific value, and low ignition energy, hydrogen could easily become a threat once it leaks and accumulates up to the combustion or explosion limit. For most safety issues with different severities, hydrogen leakage acts as a critical link in the mechanism of failures. According to the H2Tools Database [1], 83 among 220 reported hydrogen-related accidents were related to hydrogen leakage, accounting for 37.73% of the total. In fact, in other accidents, hydrogen leakage is also very likely to be one of the causes or potential consequences. Therefore, the safety risks associated with hydrogen leakage warrant further attention.

Presently, researchers mainly use computational fluid dynamic methods or gas release experiments to study the dispersion of leaking hydrogen. Based on the distribution of hydrogen in facilities, safety boundaries can be defined, and safety measures such as detection and ventilation can be designed. Simulations were carried out in confined spaces like garages and tunnels with different release pressures, leak orifice sizes, and ventilation systems, which influence the volume and distribution of flammable gas clouds [2–8]. The quantitative methods of leakage risk mainly include Bayesian models, dynamic Bayesian networks, and other statistical methods based on prior knowledge, which predict the leakage probability in the hydrogen-related field from a large number of empirical data related to the oil, gas, and chemical industry [9–11]. The conclusions drawn from such studies are mainly used to guide the structural design and accident treatment plans of hydrogen-related sites, such as the determination of the distance between hydrogen storages in a facility, personnel evacuation routes, emergency response methods, etc., which relate to pre- and post- event safety. A few studies have focused on in-event safety, using simulation or experiments to guide the design of test protocols. Tchouvelev et al. [12] compared sensors'

response at different positions under several leaking conditions. CFD was used to study the flammable gas cloud, and the results were validated by helium release experiments. Advice on sensor installation was proposed based on the consideration of minimizing the effect of ventilation on sensor response. Zhao et al. [13] used a neural network and dynamic time warping algorithm to locate the leaking position in an underground garage with distributed sensors' signal. The ANN provided predictions with 78.4% accuracy and DTW of 87.5%.

In terms of hydrogen leakage detection, the general scheme in the industrial and transportation field is to install sensors near the top side of the facility where the hydrogen system is placed, and it is expected that hydrogen will accumulate around the sensors (called spatial concentration sensors) under buoyancy and trigger an alarm. However, this type of detection can have long detection delays and may even be unresponsive to leakages due to air convection or spatial blockages. Hydrogen can accumulate away from the sensors, potentially igniting or exploding. In these scenarios, a reduction in the delay of hydrogen detection is expected to provide a safety gap for emergency measures such as ventilation, power cut-off, and evacuation. The scheme of distributed sensor placement adopted by Nakano [14] and Zhao [15] can alleviate this issue to some extent, but it may not be possible or economic to arrange a large number of spatial concentration sensors in the compact cabins of outdoor equipment, hydrogen trucks, and hydrogen fuel cell vehicles.

Although there have been many simulations and experiments on specific leakage scenarios, there are few quantitative evaluations and limited guidance on in-event safety measures such as hydrogen detection. Here, we combined hydrogen leakage simulation results and historical empirical data to propose an index to assess hydrogen sensor placement. At the same time, to address the uncertainty in response time of spatial concentration sensors, we propose near-field sensors that aim at allowing the leaked hydrogen to make immediate contact with the hydrogen sensors, to reduce the time of hydrogen flow, diffusion, and accumulation [16]. This can be achieved by designing sensor nodes that are mounted on pipeline joints, which are vulnerable to hydrogen leakages, as statistical results showed [17,18]. The proposed index was used to evaluate sensor placement and helped optimize the sensor installation scheme when using only spatial concentration sensors or spatial concentration sensors combined with multiple near-field sensors.

2. Methods

Hydrogen buses require space for luggage under the passenger cabin, and hydrogen tanks cannot be installed on the top of the buses due to their height limit. So, in the current layout, we placed the tanks inside the luggage cabin, surrounded by baffles. This layout minimized changes to the original design and left the hydrogen system in a confined space. Meanwhile, the tanks, pipelines, and valves might suffer collisions during traffic accidents. If the baffles and protecting frames are not strong enough to absorb the collision energy, these components can be deformed and fail. There were 2 groups of 4 $\times$ 134 L hydrogen tanks in the cabin. Spatial concentration hydrogen sensors were mounted on the ceiling. Nine equidistance points at the top of the cabin, aligned with the tank valves, were selected, as shown in Figure 1a, whose coordinates are listed in Table 1.

The primary issue during system failure can be leaking at the pipe junction. Indeed, the connection of pipelines is subject to great problems due to unprofessional operation and undesirable working conditions. The common bite-type joint used on vehicle hydrogen systems often suffers defects on the surface of the steel pipe or ferrule, vibration, impact, or inappropriate tightening torque, which lead to unexpected failure. Hydrogen leakage can originate between the ferrule and the steel pipe, forming a jet along the pipe at the back of the nut, as shown in Figure 1b. The pressure in the pipeline is 70 MPa on the high-pressure side and 1~2 MPa on the low-pressure side. Even if the joint fails, it is still able to prevent the free passage of gas, so the pressure of the leaking gas is reduced by throttling effect. Considering the hole diameter in previous research [19–21] and assuming that the release pressure was reduced to 20 kPa (gauge pressure), we obtained a leakage flow of 0.01 g/s

and 1 g/s for tiny and severe failure conditions. Figure 2a shows four hydrogen tanks with valves, two tee joints, and one cross joint. The 21 pipeline joints in the system were set as leakage points, and their coordinates and corresponding jet directions are shown in Table 2.

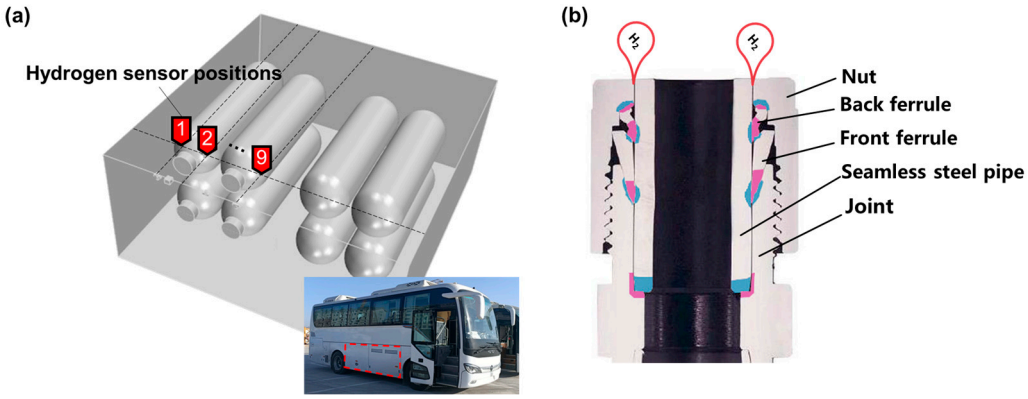

Figure 1. (**a**) Hydrogen tanks and hydrogen sensor installation in the bus. The red tags with number represented the installing positions of spatial concentration sensors (**b**) Hydrogen leak path of the double-ferrule joint.

Table 1. Positions of spatial hydrogen sensors.

Hydrogen Sensor Number	Mounting Coordinates/mm
P1	(194, 300, 1023)
P2	(294, 300, 1023)
P3	(394, 300, 1023)
P4	(494, 300, 1023)
P5	(594, 300, 1023)
P6	(694, 300, 1023)
P7	(794, 300, 1023)
P8	(894, 300, 1023)
P9	(994, 300, 1023)

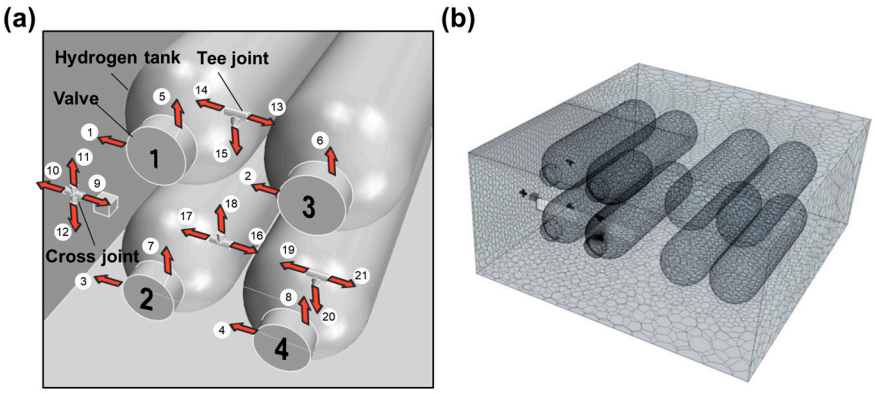

Figure 2. (**a**) Potential leakage outlets in the system. The white circles with number represented potential leaking positions. (**b**) Simulation mesh grid.

A polyhedron mesh was chosen for its robust and delicate geometry. The total number of mesh cells was 1.1×10^5 in each case, and they were refined along the jet to better simulate the hydrogen flow, as shown in Figure 2b. The grid parameters passed an independence check by comparison of the chosen mesh with grids of 8.3×10^4 and 1.4×10^5 cells, and the difference in hydrogen concentration along the jet axial line was below 5%.

Table 2. Coordinates and jet direction in the 21 leakage cases examined.

Case Number	Leakage Coordinate/mm	Jet Direction
Case 1	(287, 490, 778)	x−
Case2	(706, 490, 778)	x−
Case3	(287, 490, 278)	x−
Case4	(706, 490, 278)	x−
Case5	(414, 500, 853)	z+
Case6	(835, 500, 853)	z+
Case7	(414, 500, 353)	z+
Case8	(835, 500, 353)	z+
Case9	(124, 500, 529)	x+
Case10	(64, 500, 529)	x−
Case11	(94, 500, 558)	z+
Case12	(94, 500, 498)	z−
Case13	(604, 450, 969)	x+
Case14	(544, 450, 969)	x−
Case15	(575, 450, 938)	z−
Case16	(604, 450, 577)	x+
Case17	(544, 450, 577)	x−
Case18	(574, 450, 608)	z+
Case19	(814, 450, 577)	x−
Case20	(844, 450, 548)	z−
Case21	(874, 450, 577)	x+

The simulation used a 3D separation solver (based on pressure) and second-order upwind discretization. The SIMPLEC algorithm was used for pressure–velocity coupling. The realizable k-ε model with implicit time form, buoyancy effects, and standard wall functions was used as the turbulence model. The diffusion coefficient of hydrogen in the air was set to 6.1×10^{-5} m^2/s, and the viscosity of the hydrogen–air mixture to 1.78×10^{-5} kg/(m·s) [18]. Ansys Fluent was used for simulation for its wide application in the automotive field.

3. Results

3.1. CFD Simulation Results and Analysis

As described in Section 2, we simulated hydrogen release and dispersion in 21 cases and extracted the hydrogen concentration–time curve at the selected nine detection points. According to the National Standard for hydrogen fuel cell buses in China, GB/T 24549-2020 [22], when the volume concentration of hydrogen in a closed or semi-closed space reaches or exceeds $2 \pm 1\%$, a warning should be issued. So, we calculated the time taken, from the start of hydrogen release, to reach 1%vol hydrogen at each detection point (named trigger time). In case 21, the trigger time was longer than 120 s; so, we excluded this value from our results. The trigger time in the other 20 cases was plotted, as shown in Figure 3.

The trigger time, shown in Figure 3, varied significantly for each leak point depending on the detection point, with increasing or decreasing trends. The occurrence of opposite trends meant that there was no single sensor installation point that could monitor all cases with the shortest trigger time. For a single detection point, the response was rapid in some cases but delayed in others. The influencing factors of the trigger time were not only related to the distance between release and detection points but also affected by the direction of the jet flow and the presence of obstacles. Therefore, a sensor installation position cannot be decided only according to the distance from a potential release point. For better illustration, three typical cases were selected for detailed analysis, as shown in Figure 4.

In case 6, the hydrogen supply port of the tank valve failed, generating an upward jet flow below the detection point P7. Hydrogen dispersed radially around the ceiling. The farther the detection point was from P7, the longer the trigger time, as shown in Figure 4a. The trigger time at P1 was the longest.

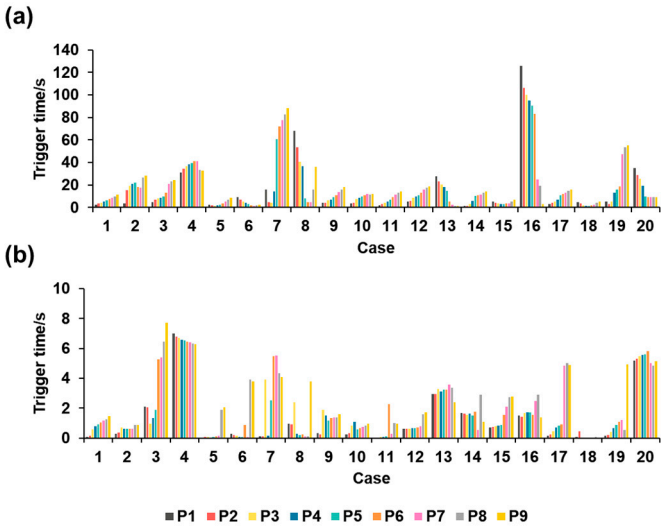

Figure 3. Hydrogen trigger time under leakage flows of (**a**) 0.01 g/s and (**b**) 1 g/s, for tiny and severe failure conditions, respectively.

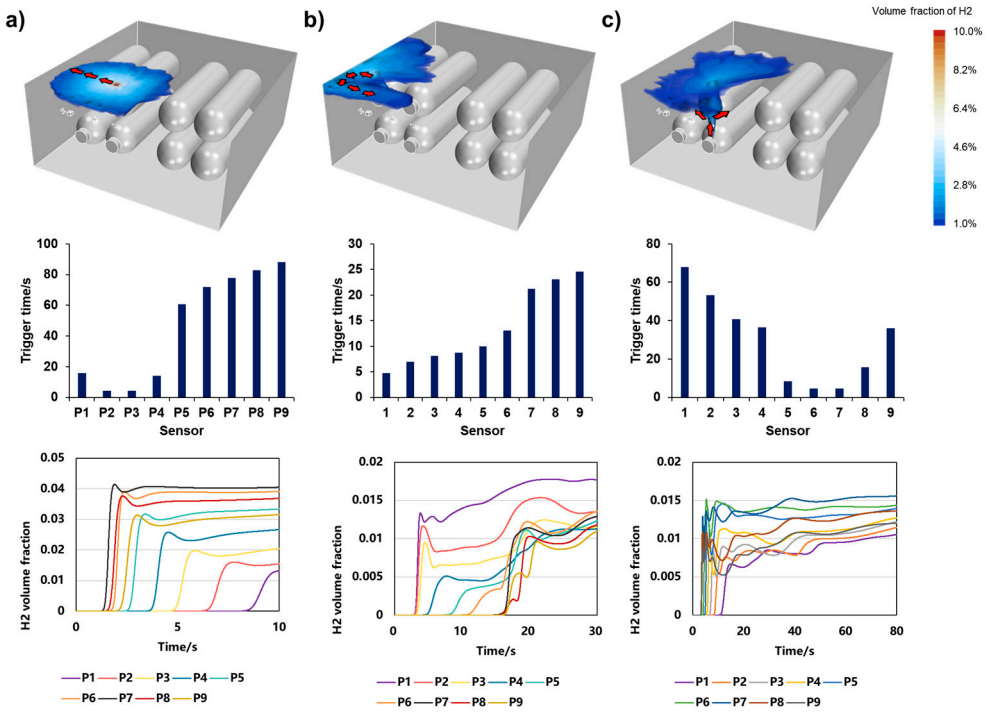

Figure 4. Three cases extracted from the CFD simulation noted as (**a**) case A, (**b**) case B, and (**c**) case C.

In case 2, hydrogen was released from the refilling port of the same valve with jet flow in the X- direction. The gas cloud moved horizontally while spreading to the top under buoyancy, and triggered P1 first. Then, the gas generated a circular flow after impinging on the side walls, finally reaching P2~P9. As can be seen from Figure 4b, the trigger time was very different from that of case 6. The detection points closer to P1 were triggered earlier, and their trigger time was generally longer than in case 6. The trigger time at P9 was the longest.

In case 8, the leakage point was farther from the ceiling, and the upward path of hydrogen was blocked by another hydrogen tank. The trend of the trigger time was similar to that of case 6, but the trigger time at P1~P4 and P8~P9 was nearly 10 times longer. As can be seen from the velocity cloud plot in Figure 4c, because of the longer upward path and

the obstruction, the velocity at the ceiling was greatly reduced, which made the dispersion very slow and led to a delay in sensor triggering.

In addition to the differences in trigger time, we also noticed that an extremely long trigger time appeared in cases 6, 16, and 19. Hydrogen concentration and velocity are shown in Figure 5. In case 6, the supply port of tank 2 leaked, similar to case 8, which further delayed the detection because of obstacles blocking the propagation of the hydrogen gas clouds.

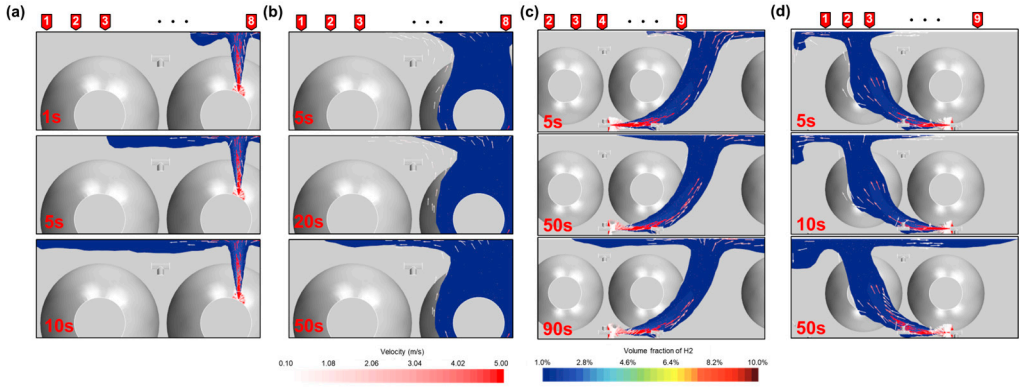

Figure 5. Hydrogen concentration profile in (**a**) case 6 (0.01 g/s), (**b**) case 8 (0.01 g/s), (**c**) case 16 (1 g/s), and (**d**) case 19 (1 g/s). The red tags represented the installing positions of spatial concentration sensors.

In case 16, the jet flow formed in the X+ direction and, so, was far away from most detection points when it reached the ceiling. Also, due to the initial velocity in the X+ direction, the flow in the X— direction was very weak; so, the trigger time at P1 was 126.08 s.

In case 19, the hydrogen jet was horizontal and encountered obstacles; so, the velocity decreased. As it rose to the ceiling, the velocity in the X— direction was maintained; so, accumulation occurred in the ceiling corner. Meanwhile, the flow in the X+ direction was very weak, resulting in a delay in P4~P9 triggering.

From the above results and analysis, we identified three factors that affected hydrogen dispersion:

1. Position of the leakage point. At the ceiling, the volume of the hydrogen cloud increased due to the continuous leakage, while hydrogen diffused radially, driven by the concentration gradient. Therefore, the trigger time of the surrounding detection points is related to the distance from the detection points to the center of the hydrogen cloud.
2. Direction of the jet. The direction of the jet affected the initial position of the gas cloud when it reached the ceiling. Vertical upward or downward jets will finally rise straightly above the leakage point, driven by buoyancy. A jet with horizontal velocity will not only move upward, but also move horizontally and impinge on the ceiling somewhere, thus deviating from the leakage area. On the other hand, the hydrogen cloud may still have a horizontal velocity when it reaches the ceiling; so, hydrogen will diffuse faster along the velocity direction and more slowly in the opposite direction.
3. Obstacles. Large obstacles will block hydrogen dispersion. Small obstacles that the gas cloud seems to be able to bypass, such as tank valves, are sometimes ignored. Although hydrogen will eventually flow around the obstacle, the speed of the flow decreases because of the boundary layer effect on the obstacle surface, resulting in an inactive dispersion, thus delaying detection.

3.2. Quantitative Assessment

As can be drawn from the previous sections, there was no single location with the fastest triggering in all situations; so, we propose a quantitative index to evaluate the average performance of all installed sensors, named average detection delay index (ADDI). The ADDI was obtained by weighting the trigger time, and the composition of the weights included the frequency of occurrence and the risk of leakages. The addition of weights prioritized leakage patterns with a higher frequency of occurrence and a greater risk of hazard expansion.

However, there currently are few hydrogen-related leakage data available; so, it was difficult to obtain consistent estimates by the traditional frequency statistical methods. Bayesian statistical methods can be used to obtain a prior distribution by combining information from multiple sources, such as petrochemical industry data, and then updating the estimates with limited hydrogen-related data to obtain a posterior distribution, which can be used as the basis for leakage frequency prediction.

$$P(N|D) = \frac{P(D|N)P(N)}{P(D)}$$

where N is the parameter to be estimated, D is the sample set, $P(N)$ is the prior estimate, $P(D \mid N)$ is likelihood, $P(N \mid D)$ is the posterior estimate, and $P(D)$ is a normalized constant.

In this work, we used the data from a two-layer Bayesian model established by Sandia National Laboratories [23]. Based on the power law relationship between leakage frequency and leakage port size, the model first took the leakage data of the general industry as a sample to estimate the leakage frequency model parameters of the general industry under different leakage port size levels, and then took the posterior estimation output of the first-layer Bayesian model as the prior estimation of the second-layer model. Finally, a small number of samples from the hydrogen-related industry were used as the input to perform incremental learning and obtain the second-layer posterior estimate. The model results are shown in Figure 6.

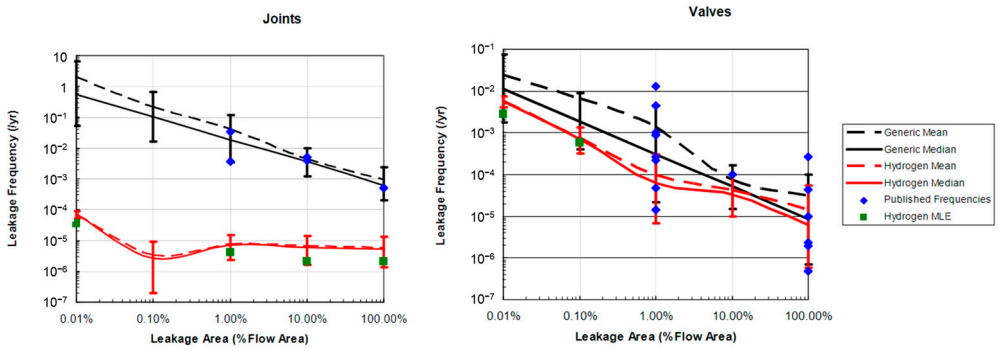

Figure 6. Leakage frequency estimated with a two-layer Bayesian model, concerning leakage from joints and valves [23].

In terms of the assessment of hazard expansion, we considered the risk of spontaneous ignition due to hydrogen jets. According to [24], spontaneous ignition is the most frequently occurring event during hydrogen leakage, while deflagration and detonation are more likely to occur in long and narrow passages, such as ventilation ducts, which are inconsistent with onboard hydrogen storage scenarios. The spontaneous ignition probability model proposed by [25] was considered, and the modeling results are shown in Figure 7.

$$h = \min\left\{1, 0.55 \times leak\ rate^{0.87}, 0.267 \times leak\ rate^{0.52}\right\}$$

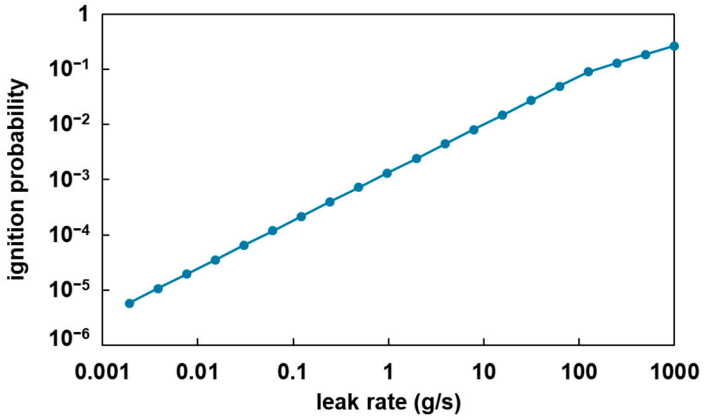

Figure 7. Ignition probability under different leak rates according to [25].

With frequency of leakage f and risk of hazard expansion h, the ADDI for a sensor installed at position j can be written as

$$ADDI_j = \sum_i f_i h_i t_{ij}$$

The leakage frequency was obtained from the joints' plot in Figure 6, and the hazard expansion risk was calculated according to [25]. t_{ij} denotes the trigger time of the detection point j in case i. When using n sensors, the expected trigger time is

$$ADDI(n) = \sum_i f_i h_i \min_j \{t_{ij}\}$$

where $\min_j \{t_{ij}\}$ denotes the minimum trigger time considering n sensor positions.

In the SNL model, leakages are classified into five levels based on the size of the leak opening. Here, we combined the five grades into two grades, which were 0.01~1% of the leakage area, corresponding to a 0.01 g/s flow, and 10~100%, corresponding to a 1 g/s flow.

Combining the CFD simulation results with the ADDI model, we first calculated the ADDI with n = 1 for nine sensor locations, as shown in Figure 8a. Placing the spatial concentration sensor at P4 led to the lowest ADDI as marked by the red rectangle in Figure 8a, i.e., detection at P4 provided the best coverage and the most rapid response to leakages with a high frequency of occurrence. The result was intuitive, for P4 was in the middle of the hydrogen tank group. For the position near P1, the ADDI was also low, mainly because the hydrogen jet spread upwards after hitting the cabin wall; so P1 could soon contact the gas mixture. The diffusion of the hydrogen plume in the P9 direction was slow, so the ADDI of P6-P9 was higher.

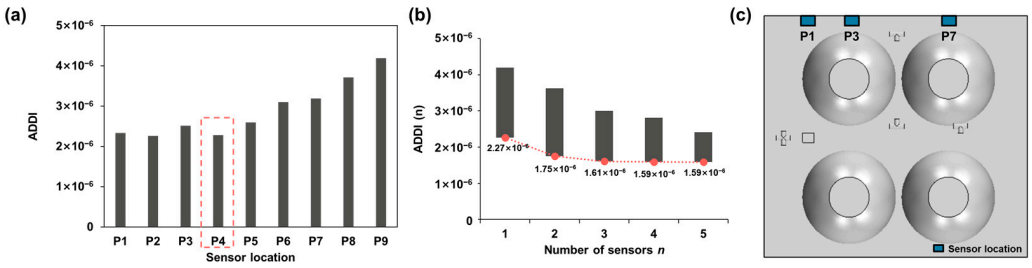

Figure 8. (**a**) The ADDI of different sensor installations, with n = 1. (**b**) ADDI range with increasing sensor number. (**c**) Optimal sensor placement.

Next, the combination of multiple sensors was evaluated, as shown in Figure 8b. The minimum ADDI decreased as the number of sensors increased, but the trend slowed down for $n > 3$. This indicates that a design with more than three sensors was redundant in this scenario. For a design with three sensors, the optimal combination was P1, P3, and P7.

Apart from the spatial concentration sensors installed at the ceiling, a new near-field hydrogen sensor was proposed in [16], which can detect the leakage of joints within 500 ms. If near-field sensors were implemented in our system, it would be possible to achieve a lower ADDI. The case of using one spatial concentration sensor with multiple near-field sensors at different locations was investigated. The trigger time of the near-field sensors was set to 0.5 s, according to [16]. The results are shown in Figure 9.

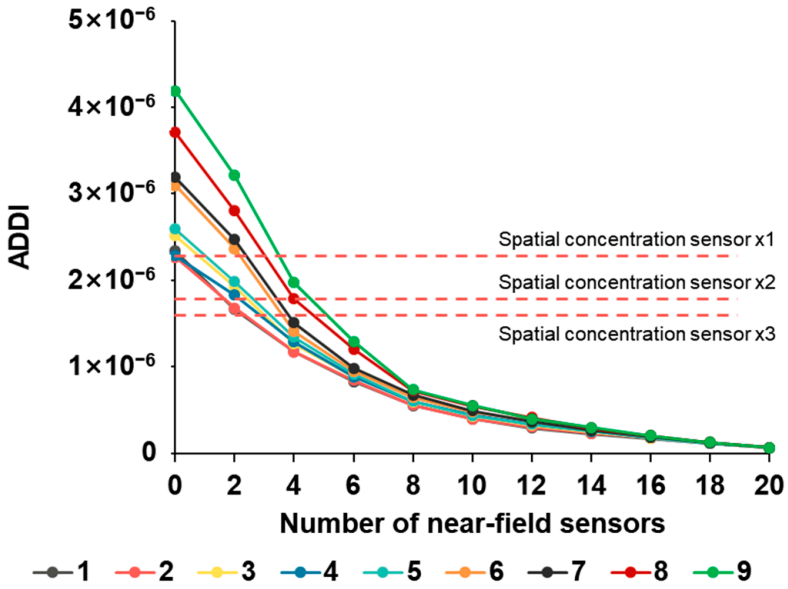

Figure 9. ADDI with different number of near-field sensors. Different curves correspond to different spatial concentration sensor placements.

As can be seen from Figure 9, the ADDI decreased as the number of near-field sensors increased. The location of the spatial concentration sensor also had a significant impact, and the best results were obtained for P1 or P2. According to the CFD simulation results, the effect of the most distant leak locations on the P1 trigger time was significantly reduced when these locations were covered by near-field sensors.

When the number of near-field sensors increased to 4–6, the ADDI of the combined detection system was lower than that of an array with three spatial concentration sensors. Considering the higher cost of spatial concentration sensors compared to that of near-field sensors, the system cost can be reduced by involving near-field sensors. Meanwhile, the lower limit of the ADDI can be reduced to under 10^{-7}, which is more than ten times lower than that in Figure 8b.

The case of four near-field sensors is illustrated in Figure 10, with two array designs using P1 and P2 as spatial concentration sensors. The blue rectangle denotes the spatial concentration sensor, and the red dots denote the near-field sensors. The numbers denote the leakage positions according to Table 2. The optimal installation locations were concentrated on the tank valves, mainly because of the high weight attributed to tank valve leakages in the frequency model.

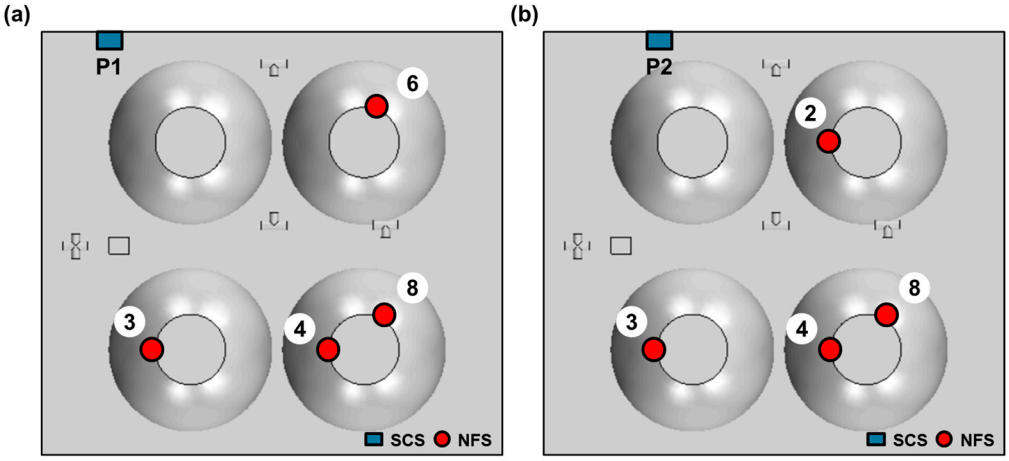

Figure 10. Sensor placement when using 1 spatial concentration sensor and 4 near-filed sensors. (**a**,**b**) gave two optimal installation with similar ADDI. The white circles with number represented the installation joints according to Table 1.

4. Conclusions

In this paper, we investigated the behavior of released hydrogen in the hydrogen storage cabin of a fuel cell coach bus. Three factors that explain the delay of hydrogen dispersion were illustrated. Then, we proposed the ADDI for evaluating the sensor array design. Using three spatial concentration sensors at P1, P3, and P7 was more reliable and efficient than using other designs. When implementing near-field sensors, the ADDI was further reduced with one spatial concentration sensor and four near-field sensors compared to that of the design with three spatial concentration sensors. The results showed the advantages of near-field sensors in composing a sensor array. Although a near-field sensor can only monitor a specific connection, its fast response and high reliability enable it to allow for an extra degree of freedom in hydrogen system safety design. However, this does not mean that spatial concentration sensors could be replaced, for their wide coverage is still needed as a second line of detection and a protective barrier.

The ADDI showed its ability to quantify the safety performances of different sensor placement schemes. However, the failure probability and risk coefficients remained uncertain and rough. With the wide spreading of hydrogen applications, the hydrogen safety issue database needs to be expanded to help with the improvement of quantitative safety assessment.

Author Contributions: Conceptualization, X.D. and J.S.; methodology, X.D.; investigation, J.S.; writing—original draft preparation, X.D.; writing—review and editing, J.S.; supervision, F.Y. and M.O. All authors have read and agreed to the published version of the manuscript.

Funding: This research was funded by the National Key Research and Development Program of China, grant number 2021YFB2501504. The APC was funded by the National Key Research and Development Program of China.

Data Availability Statement: The data presented in this study are available on request from the corresponding author.

Conflicts of Interest: The authors declare no conflicts of interest. The funders had no role in the design of the study; in the collection, analyses, or interpretation of data; in the writing of the manuscript; or in the decision to publish the results.

References

1. Pacific Northwest National Laboratory, H2TOOLS. Available online: https://h2tools.org/ (accessed on 6 December 2024).
2. Giannissi, S.G.; Shentsov, V.; Melideo, D.; Cariteau, B.; Baraldi, D.; Venetsanos, A.G.; Molkov, V. CFD benchmark on hydrogen release and dispersion in confined, naturally ventilated space with one vent. *Int. J. Hydrogen Energy* **2015**, *40*, 2415–2429. [CrossRef]

3. Xie, H.; Li, X.; Christopher, D.M. Emergency blower ventilation to disperse hydrogen leaking from a hydrogen-fueled vehicle. *Int. J. Hydrogen Energy* **2015**, *40*, 8230–8238. [CrossRef]
4. Baraldi, D.; Melideo, D.; Kotchourko, A.; Ren, K.; Yanez, J.; Jedicke, O.; Giannissi, S.G.; Tolias, I.C.; Venetsanos, A.G.; Keenan, J.; et al. Development of a model evaluation protocol for CFD analysis of hydrogen safety issues the SUSANA project. *Int. J. Hydrogen Energy* **2017**, *42*, 7633–7643. [CrossRef]
5. Li, F.; Yuan, Y.; Yan, X.; Malekian, R.; Li, Z. A study on a numerical simulation of the leakage and diffusion of hydrogen in a fuel cell ship. *Renew. Sustain. Energy Rev.* **2018**, *97*, 177–185. [CrossRef]
6. Hussein, H.; Brennan, S.; Molkov, V. Dispersion of hydrogen release in a naturally ventilated covered car park. *Int. J. Hydrogen. Energy* **2020**, *45*, 23882–23897. [CrossRef]
7. Mao, X.; Ying, R.; Yuan, Y.; Li, F.; Shen, B. Simulation and analysis of hydrogen leakage and explosion behaviors in various compartments on a hydrogen fuel cell ship. *Int. J. Hydrogen Energy* **2021**, *46*, 6857–6872. [CrossRef]
8. Li, Y.; Hou, X.; Wang, C.; Wang, Q.; Qi, W.; Li, J.; Zhang, X. Modeling and analysis of hydrogen diffusion in an enclosed fuel cell vehicle with obstacles. *Int. J. Hydrogen Energy* **2022**, *47*, 5745–5756. [CrossRef]
9. Beaucourt, J.; Georgescu, G. Modeling hydrogen explosion in level 1 Psa. In Proceedings of the PSA 2019—International Topical Meeting on Probabilistic Safety Assessment and Analysis, Charleston, SC, USA, 28 April–3 May 2019; pp. 304–309.
10. Chau, K.; Djire, A.; Vaddiraju, S.; Khan, F. Process Risk Index (PRI)—A methodology to analyze the design and operational hazards in the processing facility. *Process Saf. Environ. Prot.* **2022**, *165*, 623–632. [CrossRef]
11. Zarei, E.; Khan, F.; Yazdi, M. A dynamic risk model to analyze hydrogen infrastructure. *Int. J. Hydrogen Energy* **2021**, *46*, 4626–4643. [CrossRef]
12. Tchouvelev, A.V.; Buttner, W.J.; Melideo, D.; Baraldi, D.; Angers, B. Development of risk mitigation guidance for sensor placement inside mechanically ventilated enclosures—Phase 1. *Int. J. Hydrogen Energy* **2021**, *46*, 12439–12454. [CrossRef]
13. Chen, M.; Zhao, M.; Huang, T.; Ji, S.; Chen, L.; Chang, H.; Christopher, D.M.; Li, X. Measurements of helium distributions in a scaled-down parking garage model for unintended releases from a fuel cell vehicle. *Int. J. Hydrogen Energy* **2020**, *45*, 22166–22175. [CrossRef]
14. Nakano, S.; Goto, Y.; Yokosawa, K.; Tsukada, K. Hydrogen gas detection system prototype with wireless sensor networks. In Proceedings of the SENSORS, 2005 IEEE, Irvine, CA, USA, 30 October–3 November 2005; p. 4.
15. Zhao, M.; Huang, T.; Liu, C.; Chen, M.; Ji, S.; Christopher, D.M.; Li, X. Leak localization using distributed sensors and machine learning for hydrogen releases from a fuel cell vehicle in a parking garage. *Int. J. Hydrogen Energy* **2021**, *46*, 1420–1433. [CrossRef]
16. Deng, X.; Sun, J.; Yang, F.; Ouyang, M. Design of Long-Life Wireless Near-Field Hydrogen Gas Sensor. *Sensors* **2024**, *24*, 1332. [CrossRef] [PubMed]
17. Sakamoto, J.; Sato, R.; Nakayama, J.; Kasai, N.; Shibutani, T.; Miyake, A. Leakage-type-based analysis of accidents involving hydrogen fueling stations in Japan and USA. *Int. J. Hydrogen Energy* **2016**, *41*, 21564–21570. [CrossRef]
18. Wang, T.; Yang, F.; Hu, Q.; Hu, S.; Li, Y.; Ouyang, M. Experimental and simulation research on hydrogen leakage of double ferrule joints. *Process Saf. Environ. Prot.* **2022**, *160*, 839–846. [CrossRef]
19. Choi, J.; Hur, N.; Kang, S.; Lee, E.D.; Lee, K.B. A CFD simulation of hydrogen dispersion for the hydrogen leakage from a fuel cell vehicle in an underground parking garage. *Int. J. Hydrogen Energy* **2013**, *38*, 8084–8091. [CrossRef]
20. Liu, W.; Christopher, D.M. Dispersion of hydrogen leaking from a hydrogen fuel cell vehicle. *Int. J. Hydrogen Energy* **2015**, *40*, 16673–16682. [CrossRef]
21. Giannissi, S.G.; Tolias, I.C.; Melideo, D.; Baraldi, D.; Shentsov, V.; Makarov, D.; Molkov, V.; Venetsanos, A.G. On the CFD modelling of hydrogen dispersion at low-Reynolds number release in closed facility. *Int. J. Hydrogen Energy* **2021**, *46*, 29745–29761. [CrossRef]
22. *GB/T 24549-2020*; Fuel Cell Electric Vehicles—Safety Requirements. Standardization Administration of China: Beijing, China, 2020.
23. LaChance, J.L.; Houf, W.G.; Fluer, I.P.R.C.A.; Fluer, L.; Middleton, B. *Analyses to Support Development of Risk-Informed Separa-tion Distances for Hydrogen Codes and Standards*; Sandia National Laboratories (SNL): Albuquerque, NM, USA; Livermore, CA, USA, 2009.
24. Yang, F.; Wang, T.; Deng, X.; Dang, J.; Huang, Z.; Hu, S.; Li, Y.; Ouyang, M. Review on hydrogen safety issues: Incident statistics, hydrogen diffusion, and detonation process. *Int. J. Hydrogen Energy* **2021**, *46*, 31467–31488. [CrossRef]
25. Aarskog, F.G.; Hansen, O.R.; Strømgren, T.; Ulleberg, Ø. Concept risk assessment of a hydrogen driven high speed passenger ferry. *Int. J. Hydrogen Energy* **2020**, *45*, 1359–1372. [CrossRef]